

Supporting Information

Resettable and enzyme-free molecular logic devices for intelligent amplification detection of multiple miRNAs via catalyzed hairpin assembly

Siqi Zhang ^a, Kai-Bin Li ^a, Wei Shi ^a, Jie Zhang ^a, De-Man Han ^{a*} and Jing-Juan Xu ^b

^a Department of Chemistry, Taizhou University, Jiaojiang, 318000, China

^b State Key Laboratory of Analytical Chemistry for Life Science and Collaborative Innovation Center of Chemistry for Life Sciences, School of Chemistry and Chemical Engineering, Nanjing University, Nanjing 210023, China

*Corresponding author

E-mail: hdmtzc@126.com

Tel.: 86-576-88660353

1.1 Instruments

UV–vis absorption measurements were performed on a Cary 50 Scan UV/Vis Spectrophotometer (Varian, USA). The polyacrylamide gels electrophoresis (PAGE) was analyzed using a UV Imaging System (Tanon 3500R, China). Fluorescence measurements were carried out on a Cary Eclipse Spectrofluorometer (Varian, USA). The ultrapure water used in this work was purified by a Millipore system.

1.2 Preparation of molecular beacons modified Fe₃O₄@SiO₂@Au nanoparticles

The Fe₃O₄ nanoparticles with the size of 200 nm were prepared according to

solvothermal method¹. Then the gold nanoparticles functionalized magnetic silica microspheres ($\text{Fe}_3\text{O}_4@\text{SiO}_2@\text{Au}$) were synthesized according to Deng et al². The diameter of the magnetic beads was about 200 nm calculated by TEM measurements.

The molecular beacons modified $\text{Fe}_3\text{O}_4@\text{SiO}_2@\text{Au}$ was prepared by mixing $\text{Fe}_3\text{O}_4@\text{SiO}_2@\text{Au}$ suspension (2 mg/L) with thiol-molecular beacons (final concentration of oligonucleotides 10 μM) in PBS buffer (0.3 M NaCl, 0.2 M $\text{KH}_2\text{PO}_4/\text{K}_2\text{HPO}_4$, pH=7) under continuous shaking for 16 hours. Then the functionalized nanoparticles were magnetic separated and washed three times using Tris-HCl buffer (20 mM Tris-HCl, 200 mM KCl, 10 mM MgCl_2 , pH 8.0) to remove excess thiol-oligonucleotides. The functionalized $\text{Fe}_3\text{O}_4@\text{SiO}_2@\text{Au}$ nanocomposites were stored in the buffer solution.

1.3 Preparation MB1/MB2/H₁/H₂ complexes

The molecular beacons 1 (0.2 mg/mL) and molecular beacons 2 (0.2 mg/mL) modified $\text{Fe}_3\text{O}_4@\text{SiO}_2@\text{Au}$ (MB1 and MB2) mixed with 100 nM H₁ and H₂ were used as the platform for the bivariate analysis of miR-21 and miR-155 in this investigation, including OR and INHIBIT logic gate. The required inputs for each logic gate were added into the logic platform according to the logic operation. And the fluorescence responses of the system were recorded after adding various inputs into the platform for 2 h. The concentrations of inputs DNA/miRNA strands were 2 nM.

1.4 OR Logic Gate Composed of miR-21 and miR-155

The MB1/MB2/H₁/H₂ complexes were used as the initial platform to construct

the OR logic gate. For entry a, nothing was added to the platform. For entry b, 2 nM miR-21 was added to the platform. For entry c, 2 nM miR-155 was added to the platform. For entry d, 2 nM miR-21 and 2 nM miR-155 were simultaneously added to the platform. The samples were diluted with PBS buffer to a final volume of 500 μ L. The solution mixture was allowed to react at room temperature for 2 h before fluorescence measurement.

1.5 INHIBIT Logic Gate Composed of miR-21 and P1

The MB1/MB2/H₁/H₂ complexes were also used as the initial platform to construct the INHIBIT logic gate. For entry a, nothing was added to the platform. For entry b, 2 nM miR-21 was added to the platform. For entry c, 2 nM P1 was added to the platform. For entry d, 2 nM miR-21 and 2 nM P1 were simultaneously added to the platform. The samples were diluted with PBS buffer to a final volume of 500 μ L. The solution mixture was allowed to react at room temperature for 2 h before fluorescence measurement.

1.6 INHIBIT Logic Gate Composed of miR-155 and P2

The MB1/MB2/H₁/H₂ complexes were also used as the initial platform to construct the INHIBIT logic gate. For entry a, nothing was added to the platform. For entry b, 2 nM miR-155 was added to the platform. For entry c, 2 nM P2 was added to the platform. For entry d, 2 nM miR-155 and 2 nM P2 were simultaneously added to the platform. The samples were diluted with PBS buffer to a final volume of 500 μ L. The solution mixture was allowed to react at room temperature for 2 h before fluorescence measurement.

1.7 Preparation MB1/MB2/MB3/H₁/H₂/H₃ complexes

The molecular beacons 1, molecular beacons 2, molecular beacons 2, molecular beacons 3 modified Fe₃O₄@SiO₂@Au (MB1, MB2, MB3) mixed with H₁, H₂ and H₃ were used as the platform for the analysis of miR-21, miR-155, miR Let-7a in this investigation, including OR and INHIBIT logic gate. The required inputs for each logic gate were added into the logic platform according to the logic operation. And the fluorescence responses of the system were recorded after adding various inputs into the platform for 2 h. The concentrations of inputs DNA/miRNA strands were 2 nM.

1.8 OR Logic Gate Composed of miR-21, miR-155 and miR Let-7a

The MB1/MB2/MB3/H₁/H₂/H₃ complexes were used as the initial platform to construct the OR logic gate. For entry a, nothing was added to the platform. For entry b, 2 nM miR-21 was added to the platform. For entry c, 2 nM miR-155 was added to the platform. For entry d, 2 nM miR Let-7a was added to the platform. For entry e, 2 nM miR-21 and 2 nM miR-155 were simultaneously added to the platform. For entry f, 2 nM miR-21 and 2 nM miR Let-7a were simultaneously added to the platform. For entry g, 2 nM miR-155 and 2 nM miR Let-7a were simultaneously added to the platform. For entry h, 2 nM miR-21, 2 nM miR-155 and 2 nM miR Let-7a were simultaneously added to the platform. The samples were diluted with PBS buffer to a final volume of 500 μ L. The solution mixture was allowed to react at room temperature for 2 h before fluorescence measurement.

1.9 INHIBIT Logic Gate Composed of miR Let-7a and P3

The MB1/MB2/MB3/H₁/H₂/H₃ complexes were also used as the initial platform to construct the INHIBIT logic gate. For entry a, nothing was added to the platform. For entry b, 2 nM miR Let-7a was added to the platform. For entry c, 2 nM P3 was added to the platform. For entry d, 2 nM Let-7a and 2 nM P3 were simultaneously added to the platform. The samples were diluted with PBS buffer to a final volume of 500 μ L. The solution mixture was allowed to react at room temperature for 2 h before fluorescence measurement.

1.10 Native polyacrylamide gel electrophoresis

Polyacrylamide gel (12%) was prepared with 1 \times Tris-borate-EDTA buffer (89 mM Tris, 89 mM boric acid, 2 mM EDTA, pH 8.3). Each sample was prepared with 1 \times Tris-borate-EDTA buffer, and the concentration of each DNA/miRNA strand was 2 μ M. The sample solution was heated at 90 $^{\circ}$ C for 10 min and then annealed slowly to room temperature. 10 μ L of each sample was mixed with 6 \times loading buffer (2 μ L) before loading into the gel. The gel was run under a constant voltage of 140 V over a period of about 1 h. The gel was stained with 0.5 μ g/mL ethidium bromide (EB) solution for 0.5 h and then washed with pure water twice. Photographs were taken under UV light by using a fluorescence imaging system.

1.11 Human Serum

Human serum samples were diluted with reaction buffer 10 times prior to detection. Then, the target miRNA was detected in these serum samples following the

same procedure.

Table S1 DNA sequences used in this work

name	Base number	DNA sequences(from 5'-terminal to 3'terminal)
miRNA-21	22	UAGCUUAUCAGACUGAUGUUGA
miR-155	23	UUA AUGCUAAUCGUGAUAGGGGU
miRNA Let-7a	22	UGAGGUAGUAGGUUGUAUAGUU
MB1	48	FAM-TAGCTTATCAGACTGCCTACAGTAGATCAACATCAGTCTGATAAGCTA-SH
MB2	49	FAM-TTAATGCTAATCGTGCCTACAGTAGAACCCTATCACGATTAGCATTAA-SH
MB3	48	FAM-TGAGGTAGTAGGTTGCCATGTGTAGAACTATAACAACCTACTACCTCA-SH
H1	51	CCTACAGTAGATAGCTTATCAGACTGTAGTTGATCTACTGTAGGCAGTCTG
H2	52	CCTACAGTAGATTAATGCTAATCGTGATACGGCTTCTACTGTAGGCACGATT
H3	51	CCATGTGTAGATGAGGTAGTAGGTTGTAAAGATTCTACACATGGCAACCTA
MB1 for page (MBP1)	48	TAGCTTATCAGACTGCCTACAGTAGATCAACAT CAGTCTG-ATAAGCTA
MB2 for page (MBP2)	49	TTAATGCTAATCGTGCCTACAGTAGAACCCTATCACGATTAGCATTAA
MBP3 for page (MBP3)	48	TGAGGTAGTAGGTTGCCATGTGTAGAACTATAACAACCTACTACCTCA
miRNA-141	22	UAACACUGUCUGGUAAAGAUGG
miRNA-221	23	AGCUACAUUGUCUGCUGGGUUUC
miRNA-205	23	UCCUUCAUCCACCGGAGUCUGU

The binding affinities for the hybridized sequences are calculated using “The DINAMelt Web Server” and listed as follows.

miR-21 to MB1: $\Delta G = -25.2$ kcal/mol $\Delta H = -167.9$ kcal/mol $T_m = 72.5^\circ\text{C}$

H1 to MB1: $\Delta G = -44.3$ kcal/mol $\Delta H = -300.8$ kcal/mol $T_m = 79.6^\circ\text{C}$

According to the above, we can see the binding affinity and stability of H1 to MB1 is stronger than that of miR-21 to MB1, leading to the strand displacement amplification.

The result is in agreement with fluorescence spectra of the system and native

polyacrylamide gel analysis.

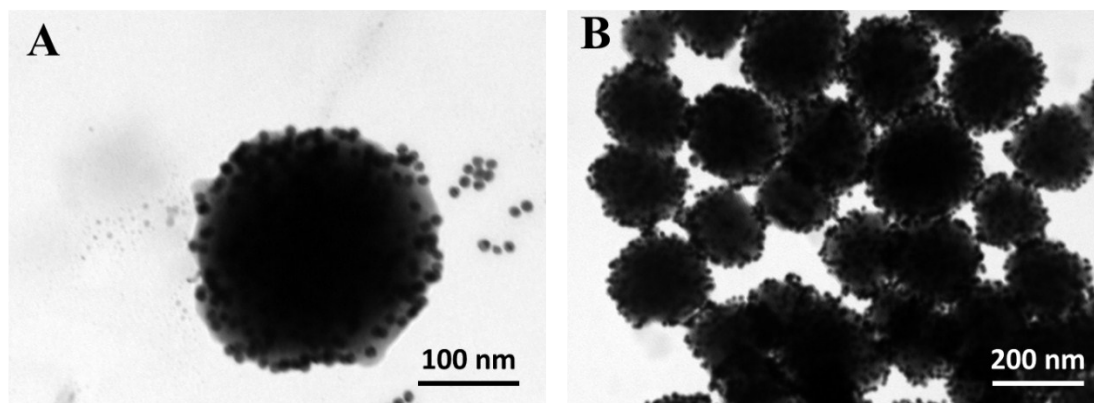


Fig. S1. Transmission electron micrograph (TEM) of magnetic $\text{Fe}_3\text{O}_4@\text{SiO}_2@\text{Au}$ nanocomposites.

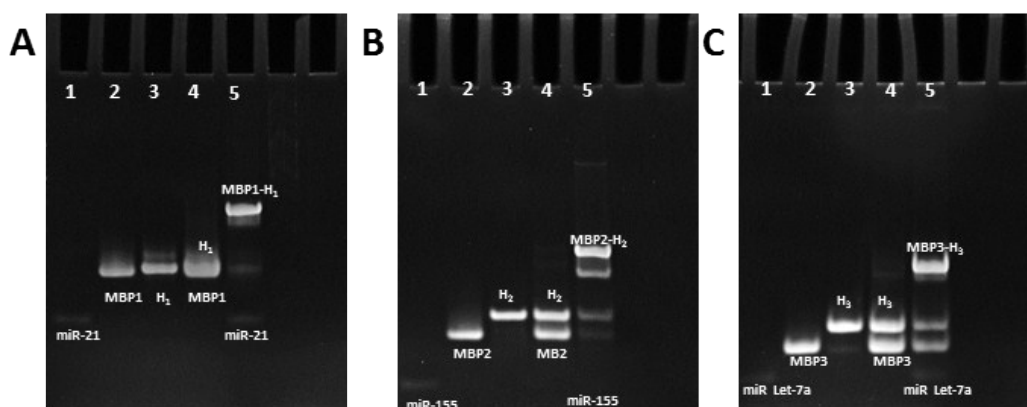


Fig. S2 (A) Native polyacrylamide gel analysis of the interactions among miR-21, MBP1 and H₁: (1) miR-21, (2) MBP1, (3)H₁, (4) MBP1+ H₁, (5) miR-21+MBP1+ H₁. (B) Native polyacrylamide gel analysis of the interactions among miR-155, MBP2 and H₂: (1) miR-155, (2) MBP2, (3)H₂, (4) MBP2+ H₂, (5) miR-155+MBP2+ H₂. (C) Native polyacrylamide gel analysis of the interactions among miR Let-7a, MBP3 and H₃: (1) miR Let-7a, (2) MBP3, (3)H₃, (4) MBP3+ H₃, (5) miR Let-7a +MBP3+ H₃. The identities of the main belts are indicated at the sides of the gel image.

PAGE analysis of the interaction among the DNA/RNA strands (miR-21, MBP1, and H₁) in the catalyzed hairpin assembly can be achieved through belt comparison. In Fig.S2A, Lanes 1–3 shows the belt location of miR-21, MBP1 and H₁. MBP1 (molecular beacon for page) is an unlabelled oligonucleotide with the same sequence of molecular beacon 1 (MB1). Significantly, after the hairpin H₁ and H₂ was mixed in TBE buffer for 2 h, there was few H₁–H₂ complexes formed (lane 4), which showed that the two hairpins H₁ and MBP1 could coexist in the buffer. After adding target miRNA (miR-21) , the DNA belt (MBP1–H₁ complexes) could be clearly seen with background intensity (lane 5), which can be concluded the hybridization with

MBP1 and H₁ took place. The results indicated that miR-21 could give rise to the self-assembly of hairpin MBP1 and H₁, which was in agreement with fluorescence spectra of the system. Similar to the catalyzed hairpin assembly of miR-21, MBP1, and H₁, the other assembly process of miR-155, MBP2, H₂ and miR Let-7a, MBP3, H₃ can be easily performed as shown in Fig. S2B and Fig. S2C.

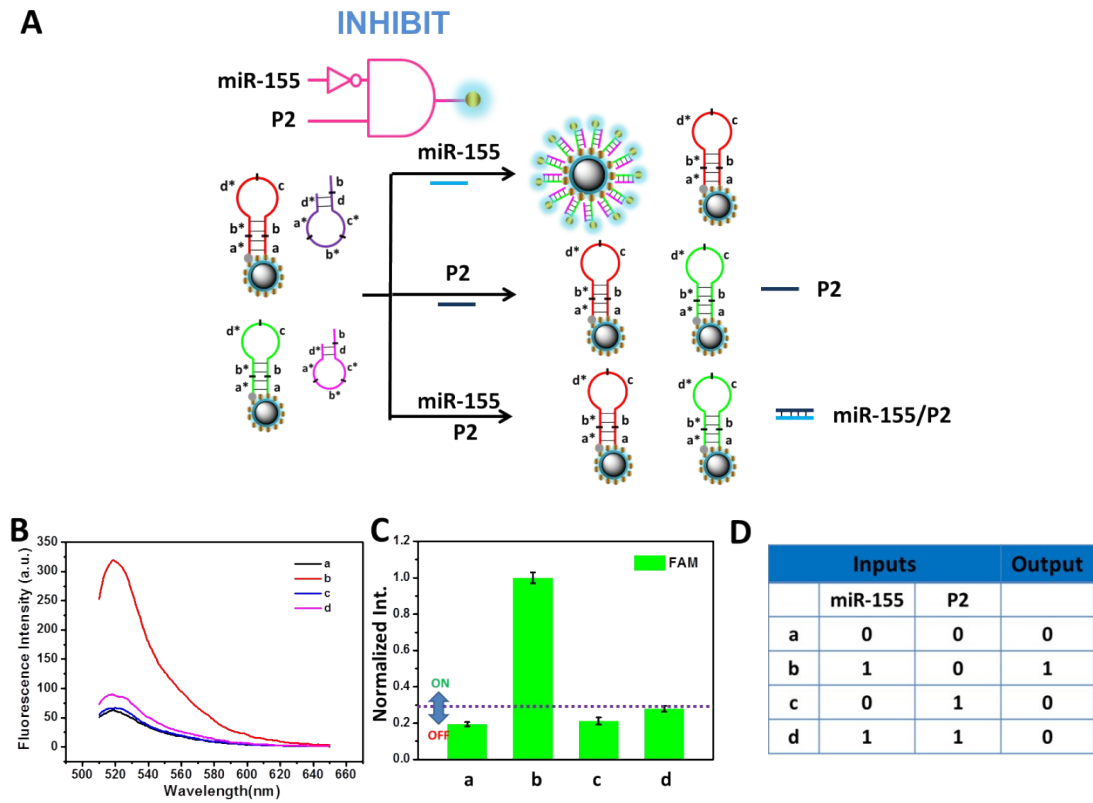


Fig. S3. (A) Schematic illustration of the INHIBIT logic gate for miR-155 and P2. (B) Fluorescence emission spectra of the FAM for INHIBIT logic gate operation in the presence of (a) MB1/MB2/H₁/H₂, (b) MB1/MB2/H₁/H₂ + miR-155, (c) MB1/MB2/H₁/H₂ + P2, and (d) MB1/MB2/H₁/H₂ + miR-155 + P2. (C) Normalized fluorescence intensity of the FAM (520 nm, green). (D) Truth table of the INHIBIT logic gate.

A

Inputs	sample	1	1	1	1	Diagnosis
	P1	0	1	0	1	
	P2	0	0	1	1	
Outputs (Fluorescence Intensity $\lambda_{Em}=520$ nm)	a	63.31	\	\	\	No target
	b	339.03	82.14	\	\	Contain miR-21
	c	325.75	323.82	83.62	\	Contain miR-155
	d	648.51	325.16	340.65	88.96	Contain miR-21 and miR-155

B

Inputs	sample	1	1	1	1	Diagnosis
	P1	0	1	0	1	
	P2	0	0	1	1	
Outputs (Normalized Intensity)	a	0.098	\	\	\	No target
	b	0.523	0.127	\	\	Contain miR-21
	c	0.502	0.499	0.127	\	Contain miR-155
	d	1	0.501	0.525	0.137	Contain miR-21 and miR-155

Threshold value=0.3

Fig. S4. Fluorescence intensity (A) and normalized fluorescence intensity (B) of combinatorial logic gates for the intelligent detection of miR-21 and miR-155 according to the input order in Fig. 4

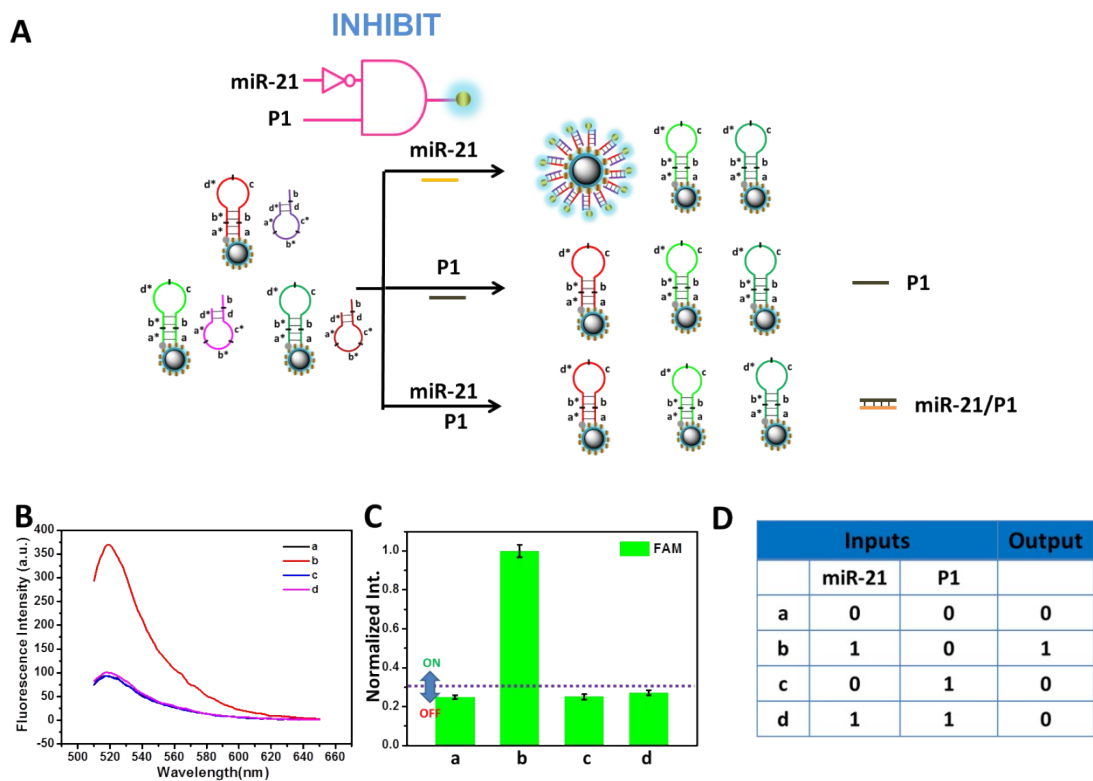


Fig. S5. (A) Schematic illustration of the INHIBIT logic gate for miR-21 and P1. (B) Fluorescence emission spectra of the FAM for INHIBIT logic gate operation in the presence of (a) MB1/MB2/MB3/H₁/H₂/H₃, (b) MB1/MB2/MB3/H₁/H₂/H₃ + miR-21, (c) MB1/MB2/MB3/H₁/H₂/H₃ +P1, and (d) MB1/MB2/MB3/H₁/H₂/H₃+ miR-21 +P1. (C) Normalized fluorescence intensity of the FAM (520 nm, green). (D) Truth table of the INHIBIT logic gate.

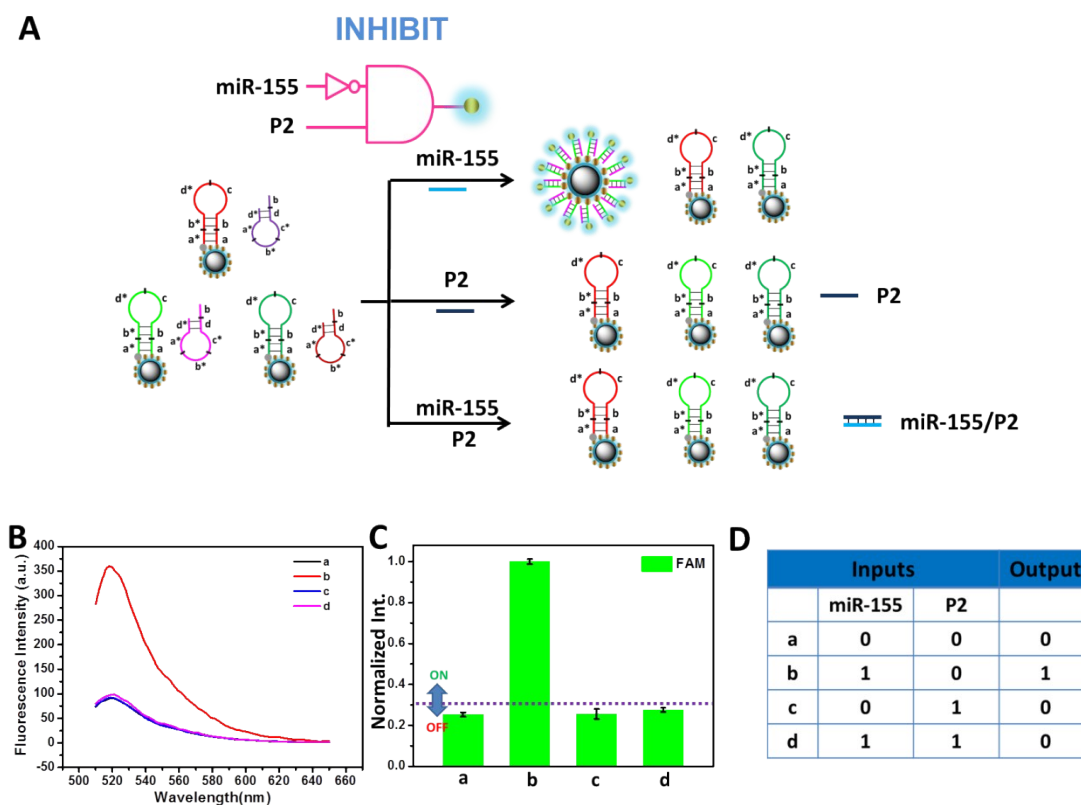


Fig. S6. (A) Schematic illustration of the INHIBIT logic gate for miR-155 and P2. (B) Fluorescence emission spectra of the FAM for INHIBIT logic gate operation in the presence of (a) MB1/MB2/MB3/H₁/H₂/H₃, (b) MB1/MB2/MB3/H₁/H₂/H₃ + miR-155, (c) MB1/MB2/MB3/H₁/H₂/H₃ +P2, and (d) MB1/MB2/MB3/H₁/H₂/H₃+ miR-155 +P2. (C) Normalized fluorescence intensity of the FAM (520 nm, green). (D) Truth table of the INHIBIT logic gate.

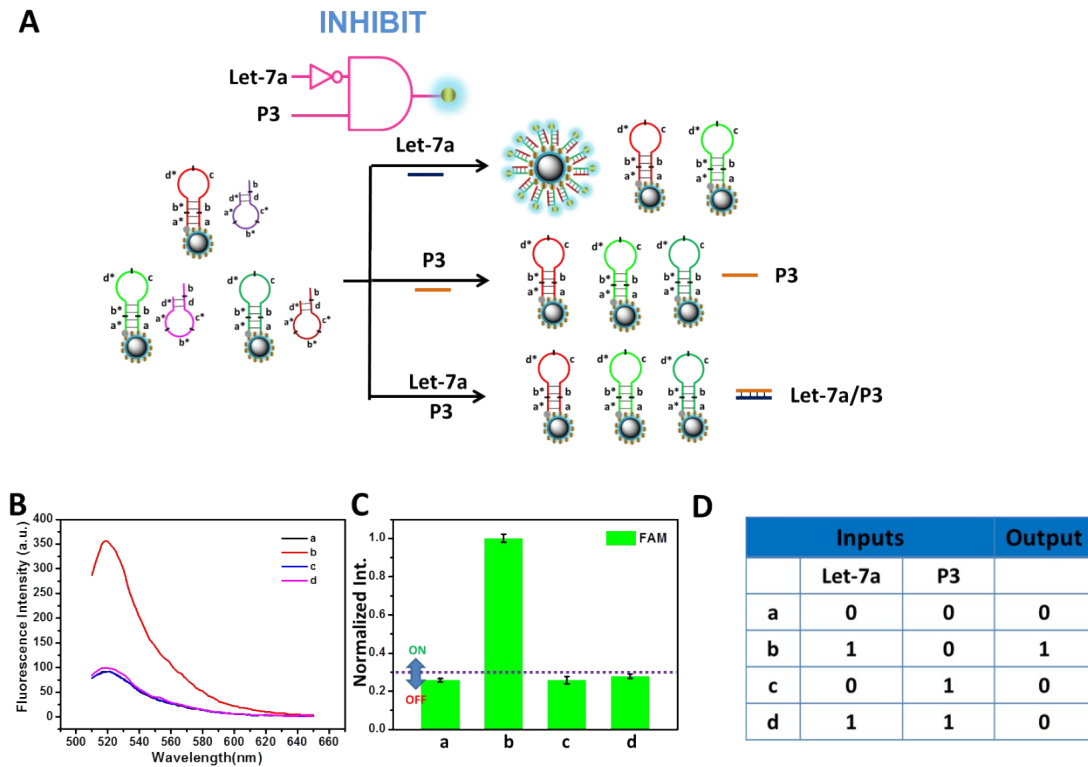


Fig. S7. (A) Schematic illustration of the INHIBIT logic gate for miR Let-7a and P3. (B) Fluorescence emission spectra of the FAM for INHIBIT logic gate operation in the presence of (a) MB1/MB2/MB3/H₁/H₂/H₃, (b) MB1/MB2/MB3/H₁/H₂/H₃ + miR Let-7a, (c) MB1/MB2/MB3/H₁/H₂/H₃ +P3, and (d) MB1/MB2/MB3/H₁/H₂/H₃+ miR Let-7a +P3. (C) Normalized fluorescence intensity of the FAM (520 nm, green). (D) Truth table of the INHIBIT logic gate.

A

Inputs	sample	1	1	1	1	1	1	1	1	Diagnosis
	P1	0	1	0	0	1	1	0	1	
	P2	0	0	1	0	1	0	1	1	
	P3	0	0	0	1	0	1	1	1	
Outputs (Fluorescence Intensity $\lambda_{Em}=520$ nm)	a	90.12	\	\	\	\	\	\	\	No target
	b	365.58	102.65	\	\	\	\	\	\	Contain miR-21
	c	350.24	352.36	98.65	\	\	\	\	\	Contain miR-155
	d	354.23	357.63	356.31	98.67	\	\	\	\	Contain miR Let-7a
	e	686.32	354.60	360.52	688.85	108.69	\	\	\	Contain miR-21 and miR-155
	f	653.96	358.22	655.39	367.61	358.36	109.76	\	\	Contain miR-21 and miR Let-7a
	g	664.35	662.37	357.28	354.28	357.64	354.38	106.49	\	Contain miR-155 and miR Let-7a
	h	904.36	665.35	654.38	689.67	361.53	361.35	375.96	115.72	Contain miR-21, miR-155 and miR Let-7a

B

Inputs	sample	1	1	1	1	1	1	1	1	Diagnosis
	P1	0	1	0	0	1	1	0	1	
	P2	0	0	1	0	1	0	1	1	
	P3	0	0	0	1	0	1	1	1	
Outputs (Normalized Intensity)	a	0.0997	\	\	\	\	\	\	\	No target
	b	0.404	0.114	\	\	\	\	\	\	Contain miR-21
	c	0.387	0.389	0.109	\	\	\	\	\	Contain miR-155
	d	0.392	0.395	0.394	0.109	\	\	\	\	Contain miR Let-7a
	e	0.759	0.392	0.399	0.762	0.120	\	\	\	Contain miR-21 and miR-155
	f	0.723	0.396	0.725	0.406	0.396	0.121	\	\	Contain miR-21 and miR Let-7a
	g	0.735	0.732	0.395	0.392	0.395	0.392	0.118	\	Contain miR-155 and miR Let-7a
	h	1	0.736	0.724	0.763	0.399	0.399	0.416	0.128	Contain miR-21, miR-155 and miR Let-7a

Threshold value=0.3

Fig. S8. Fluorescence intensity (A) and normalized fluorescence intensity (B) of combinatorial logic gates for the intelligent detection of miR-21, miR-155 and miR Let-7a according to the input order in Fig. 6

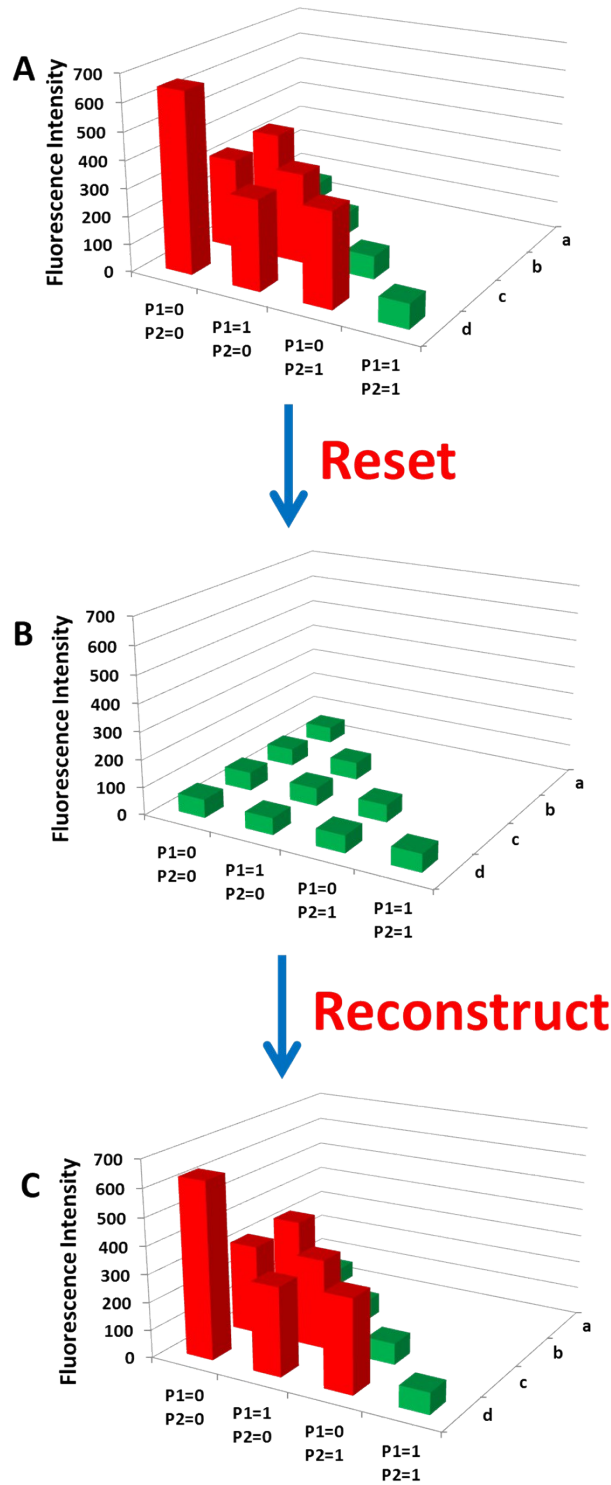


Fig. S9 Reset and reconfiguration cycles of bivariate analysis as triggered by thermal denaturation and magnetic separation.

Table S2. Results of the recovery test of miRNA in 10% human serum.

Samples	miRNA added (nM)	found (nM)	recovery (%)
miR-21	2	1.91	95.5
miR-155	2	1.95	97.5
miR Let-7a	2	1.97	98.5

Table S3. The detection limits of sensing platform for miRNA.

Sensing method	Limit of Detection	Reference
Gold Nanoparticle and Graphene Oxide	1.74 nM	[3]
Composite Probes Based Sensor		
Graphene Oxide Enhanced Fluorescence	47 pM	[4]
Anisotropy Assay		
On-Line Solid-Phase Extraction-Capillary	10 nM	[5]
Electrophoresis-Mass Spectrometry		
DNA-grafted Hemin for miRNA-21 detection	0.17 nM	[6]
Multiplexed analysis of miRNA	9.87 pM	This work

Reference:

1. S. Xuan, Y.-X. J. Wang, J. C. Yu and K. C.-F. Leung, *Chemistry of Materials*, 2009, **21**, 5079-5087.
2. X. Deng, K. Lin, X. Chen, Q. Guo and P. Yao, *Chemical Engineering Journal*, 2013, **225**, 656-663.
3. M. Hong, H. X. Sun, L. D. Xu, Q. L. Yue, G. D. Shen, M. F. Li, B. Tang and C. Z. Li, *Anal. Chim. Acta*, 2018, **1021**, 129-139.
4. S. J. Zhen, X. Xiao, C. H. Li and C. Z. Huang, *Analytical chemistry*, 2017, **89**, 8766-8771.
5. R. Pero-Gascon, V. Sanz-Nebot, M. V. Berezovski and F. Benavente, *Analytical chemistry*, 2018, **90**, 6618-6625.
6. J. Li, T. X. Yuan, T. T. Yang, L. L. Xu, L. T. Zhang, L. Z. Huang, W. Cheng

and S. J. Ding, *Sensors and Actuators B-Chemical*, 2018, **271**, 239-246.

1.12 Comparison Study between Logic Diagnosis and Separately Diagnose Each miRNA

To make our proposed sensing strategy more convincing, a comparison study between logic diagnosis and separately diagnose each miRNA is provided below. A sample which contains 2 nM miR-21, 0 nM miR-155 and 2 nM miR Let-7a is prepared as a proof of concept.

Separately diagnose each miRNA

To separately diagnose each miRNA, the three sensing platforms for miR-21, miR-155 and miR Let-7a were prepared, respectively.

Preparation MB1/ H₁ complexes: The molecular beacons 1 (0.2 mg/mL) modified Fe₃O₄@SiO₂@Au (MB1) mixed with 100 nM H₁ were used as the platform for detecting miR-21.

Preparation MB2/ H₂ complexes: The molecular beacons 2 (0.2 mg/mL) modified Fe₃O₄@SiO₂@Au (MB2) mixed with 100 nM H₂ were used as the platform for detecting miR-155.

Preparation MB3/H₃ complexes: The molecular beacons 3 (0.2 mg/mL) modified Fe₃O₄@SiO₂@Au (MB3) mixed with 100 nM H₃ were used as the platform for detecting miR Let-7a.

And the fluorescence intensity changes of the MB2/H₂ or MB3/H₃ complex upon addition of different concentrations of miR-155 or miR Let-7a was also investigated.

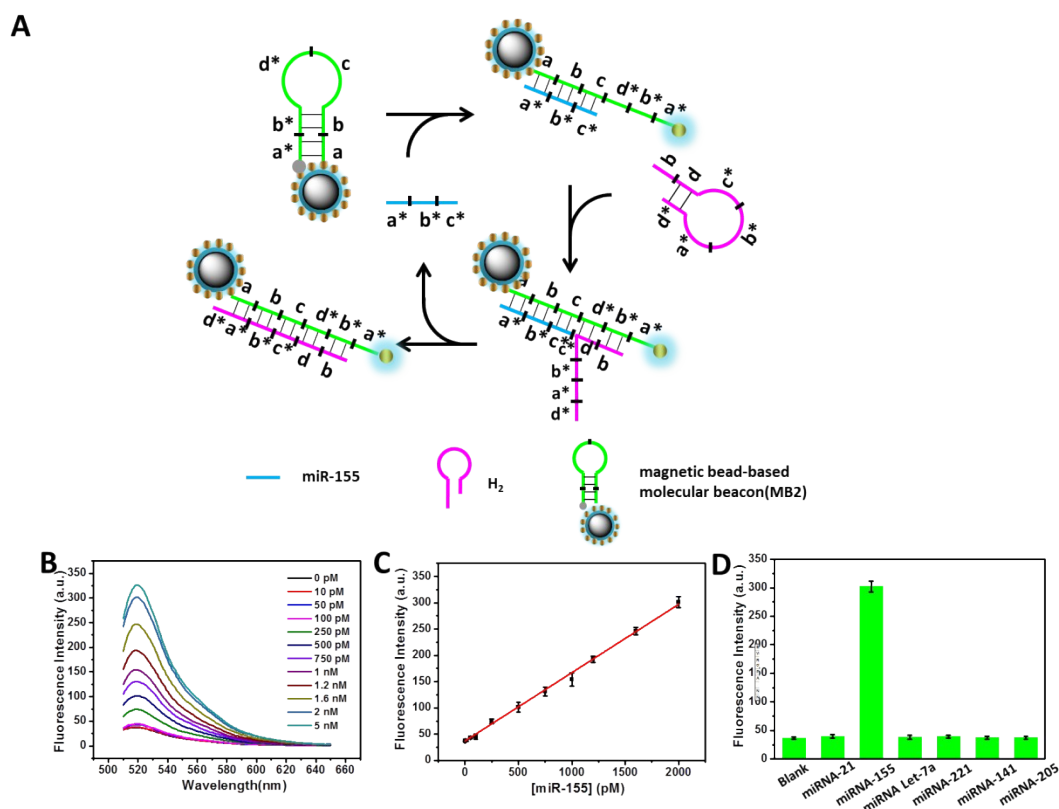


Fig. S11. (A) Schematic illustration of the CHA-based miRNA assay for the detection of miR-155. Domain are marked by alphabets and their complementary parts are denoted by asterisks. The green point represents the fluorophore (FAM). (B) Fluorescence spectra of the CHA/magnetic beads sensing platform in the presence of increasing concentrations of miR-155 from 10 pM to 5 nM. Experimental conditions: [MB2-magnetic beads] = 0.2 mg/mL, [H₂] = 100 nM. (C) The fluorescence intensity responses at 520 nm to increasing concentrations of miR-155 from 10 pM to 2 nM. (D) Histogram of the fluorescence intensity of the CHA/magnetic bead sensing platform in the presence of 2 nM miRNA-21, miRNA 155, miRNA Let-7a, miRNA-221, miRNA-141, and miRNA-205.

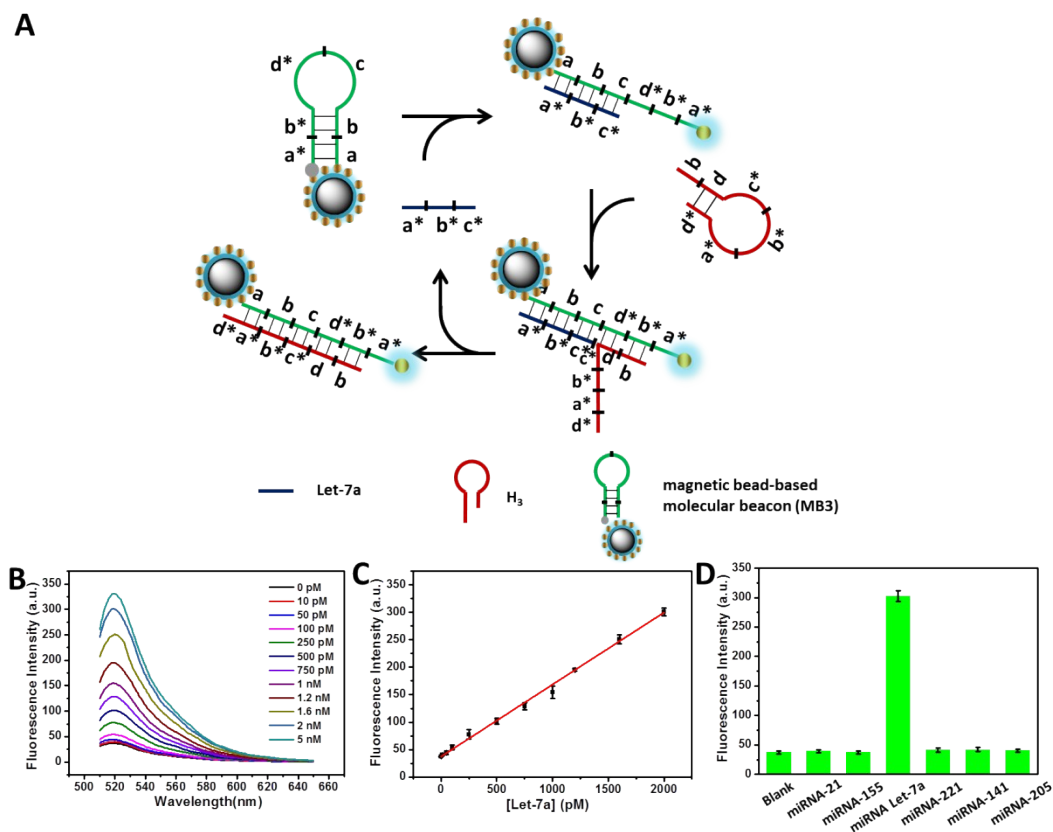


Fig. S12. (A) Schematic illustration of the CHA-based miRNA assay for the detection of miR Let-7a. Domain are marked by alphabets and their complementary parts are denoted by asterisks. The green point represents the fluorophore (FAM). (B) Fluorescence spectra of the CHA/magnetic beads sensing platform in the presence of increasing concentrations of miR Let-7a from 10 pM to 5 nM. Experimental conditions: [MB3-magnetic beads] = 0.2 mg/mL, [H₃] = 100 nM. (C) The fluorescence intensity responses at 520 nm to increasing concentrations of miR Let-7a from 10 pM to 2 nM. (D) Histogram of the fluorescence intensity of the CHA/magnetic bead sensing platform in the presence of 2 nM miRNA-21, miRNA 155, miRNA Let-7a, miRNA-221, miRNA-141, and miRNA-205.

The sample was added into the three sensing platform, respectively. And the obtained

fluorescence signal are 320.49, 98.73 and 312.85, respectively. Thus, the diagnostic result for the sample is that the sample contain miR-21 (≥ 2 nM) and miR Let-7a (≥ 2 nM), but not miR-155 (≥ 2 nM).

Diagnose by molecular logic devices

The magnetic beads modified with corresponding molecular beacons (MB1, MB2, and MB3) and mixed with H₁, H₂, and H₃ served as the initial platform. As shown in Figure 6, we input the sample to the sensing platform (MB1/MB2/MB3/ and H₁/H₂/H₃). As shown in the first column in Fig. S13, the fluorescence signal was high (see item a: FI= 657.43, NI \geq 0.3), indicating the sample contains target miRNA and triggers the CHA reaction. Nevertheless, we were unable to differentiate the miRNAs present in the sample. In such situations, conclusions can be made with the help of INHIBT logic gates. The P1 and sample were added into the biosensing system together. As shown in the second column in Fig. S13, the fluorescence signal was high (see item b: FI= 381.81, NI \geq 0.3), indicating the sample contains at least either of miR-155 or miR Let-7a. Then, P2 and the sample should be added simultaneously. As shown in the third column in Fig. S13, the fluorescence signal was high (see item c: FI= 656.34, NI \geq 0.3), indicating the sample contains at least either of miR-21 or miR Let-7a. Afterwards, P3 and the sample should be added simultaneously. As shown in the forth column in Fig. S13, the fluorescence signal was also high (see item d: FI= 389.56, NI \geq 0.3), indicating the sample contains at least either of miR-21 or miR-155. From the discussion above, a low fluorescence signal cannot be observed by only

adding one inputs. So the sample and two inputs were introduced into the the sensing platform. As shown in the fifth column in Fig. S13, the fluorescence signal was high (see item e: FI= 383.58, NI \geq 0.3), indicating the sample contains at least miR Let-7a. In the case that a low fluorescence signal can only be obtained by simultaneously addition of P1, P3 (as shown in the sixth column in Fig. S13), and the sample (see item f: FI= 102.75, NI \leq 0.3 in Fig. S13), this indicated there were both miR-21 and miR Let-7a present in the sample, because miR-21 and miR Let-7a were blocked by their complementary sequences (P1 and P3), respectively. Thus, the diagnostic results for the sample is that the sample contain miR-21 (\geq 2 nM) and miR Let-7a (\geq 2 nM), but not miR-155 (\geq 2 nM).

A

Inputs	sample	1	1	1	1	1	1	1	1	Diagnosis
	P1	0	1	0	0	1	1	0	1	
	P2	0	0	1	0	1	0	1	1	
	P3	0	0	0	1	0	1	1	1	
Outputs (Fluorescence Intensity $\lambda_{Em}=520$ nm)	a	657.43	\	\	\	\	\	\	\	No target ✕
	b	\	381.81	\	\	\	\	\	\	Contain miR-21 ✕
	c	\	\	656.34	\	\	\	\	\	Contain miR-155 ✕
	d	\	\	\	389.56	\	\	\	\	Contain miR Let-7a ✕
	e	\	\	\	\	383.58	\	\	\	Contain miR-21 and miR-155 ✕
	f	\	\	\	\	\	102.75	\	\	Contain miR-21 and miR Let-7a ✓
	g	\	\	\	\	\	\	\	\	Contain miR-155 and miR Let-7a ✕
	h	\	\	\	\	\	\	\	\	Contain miR-21, miR-155 and miR Let-7a ✕

B

Inputs	sample	1	1	1	1	1	1	1	1	Diagnosis
	P1	0	1	0	0	1	1	0	1	
	P2	0	0	1	0	1	0	1	1	
	P3	0	0	0	1	0	1	1	1	
Outputs (Normalized Intensity)	a	1	\	\	\	\	\	\	\	No target ✕
	b	\	0.581	\	\	\	\	\	\	Contain miR-21 ✕
	c	\	\	0.998	\	\	\	\	\	Contain miR-155 ✕
	d	\	\	\	0.593	\	\	\	\	Contain miR Let-7a ✕
	e	\	\	\	\	0.583	\	\	\	Contain miR-21 and miR-155 ✕
	f	\	\	\	\	\	0.156	\	\	Contain miR-21 and miR Let-7a ✓
	g	\	\	\	\	\	\	\	\	Contain miR-155 and miR Let-7a ✕
	h	\	\	\	\	\	\	\	\	Contain miR-21, miR-155 and miR Let-7a ✕

Threshold value=0.3

Fig. S13. Fluorescence intensity (A) and normalized fluorescence intensity (B) of combinatorial logic gates for the intelligent detection for a sample which contains 2 nM miR-21, 0 nM miR-155 and 2 nM miR Let-7a. The “\” symbol means that the corresponding condition can be omitted.

The reason we need such a multiplex logic gate detection system and the superiorities of such a complex system compared to apply them separately to detect each miRNA:

As shown above, the multiplex logic gate detection system can detect three miRNAs in a universal DNA-based platform as well as the same threshold

setpoint, while singular detection system (separately to detect each miRNA) needs to use different sensing platform to complete the diagnosis. Multiplexed analysis in a universal platform is highly important to execute large-scale and programmed disease screening. If the developed detection system combined within a microfluidic chip, it can implement an enormous number of miRNA detection simultaneously, greatly enhancing the processing ability of the high-throughput detection techniques and providing a possible way to achieve the high throughput screening of various diseases. The multiplex logic gate detection system can push forward the development of intelligent multi-analytes sensing and information processing at molecular level, which can be used as medical device for specific diagnostic or therapeutic functions.